PCCP

PAPER

Cite this: *Phys. Chem. Chem. Phys.*, 2016, **18**, 17983

Ultrafast differential flexibility of Cro-protein binding domains of two operator DNAs with different sequences

Susobhan Choudhury,[a] Basusree Ghosh,[b] Priya Singh,[a] Raka Ghosh,[b] Siddhartha Roy[b] and Samir Kumar Pal*[a]

Received 15th April 2016,
Accepted 3rd June 2016

DOI: 10.1039/c6cp02522f

www.rsc.org/pccp

The nature of the interface of specific protein–DNA complexes has attracted immense interest in contemporary molecular biology. Although extensive studies on the role of flexibility of DNA in the specific interaction in the genetic regulatory activity of lambda Cro (Cro-protein) have been performed, the exploration of quantitative features remains deficient. In this study, we have mutated (site directed mutagenesis: SDM) Cro-protein at the 37th position with a cysteine residue (G37C) retaining the functional integrity of the protein and labelled the cysteine residue, which is close to the interface, with a fluorescent probe (AEDANS), for the investigation of its interface with operator DNAs (O_R3 and O_R2). We have employed picosecond resolved polarization gated fluorescence spectroscopy and the well known strategy of solvation dynamics for the exploration of physical motions of the fluorescent probes and associated environments, respectively. Even though this particular probe on the protein (AEDANS) shows marginal changes in its structural flexibility upon interaction with the DNAs, a non-covalent DNA bound probe (DAPI), which binds to the minor groove, shows a major differential alteration in the dynamical flexibility in the O_R3–Cro complex when compared to that of the O_R2 complex with the Cro-protein. We attempt to correlate the observed significant structural fluctuation of the Cro-protein binding domain of O_R3 for the specificity of the protein to the operator DNA.

Introduction

Protein–DNA interaction has been explored extensively without fully understanding the forces that impart specificity.[1,2] The role of allostery in the specific protein–DNA interaction driven control of gene expression is well documented in the literature.[3–7] Dynamically driven allostery appears to be more crucial.[8–10] In a series of studies from our group, we have established that λ-repressor and Gal-repressor show altered ultrafast dynamical motions in the C-terminal domain upon operator DNA-binding in the distant N-terminal domain.[11–14] The dynamics of hydration of operator DNAs are also found to play a key role in the specific protein–DNA interaction.[15–19]

In an earlier study,[20] it was concluded that the flexibility of a target DNA may also be important for the specific DNA binding affinity. Mobility of the lac-repressor binding domain of a target DNA has been indirectly demonstrated by the observation of a mixture of B_I and B_{II} configurations about a phosphate group of the DNA moiety.[21] Although the mobility in terms of a mixture of B_I and B_{II}[22] was found to be intact upon wild type protein (lac-repressor) binding, a significant change in DNA mobility was observed in the target DNA upon complexation with the mutant lac-repressor (Y7I) protein. For the Cro-protein, the increased DNA flexibility of the binding domain with CAC-bases of an operator O_R3 has been reported.[20] In the case of complexation of mutant Cro-protein (V55C) the DNA flexibility of the operator DNA has been found to be significantly reduced.[23]

In the above historical context it is known that DNA flexibility plays a key role in the specific interaction with protein. However, till date the direct measurement of the flexibility of the specific protein binding region of a DNA in order to quantify the time scales associated with the flexibility has been sparsely reported in the literature and is the motive of our present work. In the present study, we have introduced a cysteine residue into the N-terminal half of the Cro-protein dimer[24] through site directed mutagenesis (G37C) and labeled the cysteine residue with the probe (5-((((2-iodoacetyl)amino)ethyl)amino)naphthalene-1-sulfonic acid) (IAEDANS). Polarization gated fluorescence of the probe reveals complexation of the protein upon specific interaction with different operator DNAs (O_R3 and O_R2). The strategy of

[a] *Department of Chemical, Biological & Macromolecular Sciences, S. N. Bose National Centre for Basic Sciences, Block JD, Sector III, SaltLake, Kolkata 700 098, India. E-mail: skpal@bose.res.in*

[b] *Division of Structural Biology and Bioinformatics, Indian Institute of Chemical Biology, 4, Raja S.C. Mullick Road, Kolkata 700 032, India*

investigating the dynamical time scales in the DNA minor grooves upon interaction with a specific protein using time-resolved studied is well documented.[15,25] Polarization gated picosecond resolved fluorescence studies of DAPI (4′,6-diamidino-2-phenylindole) in the minor grooves of the operator DNAs have been employed to observe the significant change in the physical motions of the probe in the operator DNAs upon interaction with the Cro-protein dimer. Picosecond resolved Stokes shifts (TRES) of the well-known solvation probe DAPI in the DNA have been followed for the investigation of the environmental dynamics in the proximity of the probe.[25] The interactions of the Cro-protein with different operator DNA sequences are found to alter the significant domain fluctuation (hundreds of picosecond to nanosecond time scales) in O_R3 compared to that of the O_R2, which has crucial importance in the gene regulatory network.

Materials and methods

Acrylamide, ampicillin, Coomassie brilliant blue, PMSF, reduced glutathione, and poly(ethyleneimine) were purchased from Sigma Chemical Co. (St. Louis, MO). Bacto-agar and yeast extract were purchased from Difco Laboratories (Detroit, MI). β-Mercaptoethanol and glycerol were purchased from Aldrich Chemical Co. (Milwaukee, WI). Thrombin, glutathione-Sepharose, benzamidine-Sepharose, and the pre-packed FPLC mono-S column were from GE Healthcare (Buckinghamshire, UK). Isopropyl β-D-thiogalactopyranoside (IPTG) was from Sisco Research Laboratories Pvt. Ltd (Mumbai, India). IAEDANS (5-((((2-iodoacetyl)amino)ethyl)amino)naphthalene-1-sulfonic acid) and DAPI (4′,6-diamidino-2-phenylindole) were purchased from Molecular Probes (ThermoFisher Scientific). All other reagents were of analytical grade quality. O_R3 (5′-TATC ACCGCAAGGGATA-3′) and its complementary oligonucleotide, and O_R2 (5′-TACAACACGCACGGTGTTAT-3′) and its complementary oligonucleotide were purchased from Trilink Technologies (San Diego, CA, USA). The oligonucleotides were mixed at a 1 : 1 molar ratio and were annealed in 0.1 M phosphate buffer of pH 8 by incubating in boiling water and then cooling slowly to room temperature.

Site directed mutagenesis (SDM)

The point mutant of Cro-protein, CroG37C, was made by site-directed mutagenesis (QuikChange II XL site-directed mutagenesis kit; Stratagene) as per the manufacturer's instructions. The mutant was confirmed by sequencing. Expression and purification of the mutant protein was carried out as described for wild-type protein below.

Protein purification and labeling with IAEDANS

Full length Cro (Enterobacteria phage lambda) cDNA was cloned in-frame into the EcoR1 and Sal1 site located downstream of the GST gene in the pGEX-4T-1 vector. Then the vector was transformed into BL21 cells and the cells were grown in Luria broth containing 100 μg ml^{-1} ampicillin at 37 °C until A_{600} reached 0.5–0.6. After that cells were induced by 1 mM IPTG for 5 h at 32 °C. Cells were harvested by centrifugation. The cell pellet was suspended in lysis buffer (50 mM Tris–HCl, 500 mM NaCl, 5 mM EDTA, 10% glycerol, pH 8.6 and 1 mM PMSF). After sonication on ice, the lysate was cleared by centrifugation (14 000 rpm, 45 min, 4 °C). The supernatant was loaded onto a GST-Sepharose (GE Healthcare) column that was pre-equilibrated with lysis buffer. The column was washed subsequently with lysis buffer and wash buffer (50 mM Tris–HCl, 200 mM NaCl, 10% glycerol, pH 8.6). The GST-tagged fusion protein was eluted with elution buffer (30 mM reduced glutathione, 50 mM Tris–HCl, 100 mM NaCl, 10% glycerol, pH 8.6). Then the protein was dialysed with 50 mM Tris–HCl, 100 mM NaCl, 10% glycerol, pH 8.6 and digested with thrombin at 16 °C for 1.5 h and loaded onto a benzamidine-Sepharose (GE Healthcare) column which was pre-equilibrated with 50 mM Tris–HCl, 100 mM NaCl, 10% glycerol, pH 8.6 for removal of thrombin. The digested protein was then further purified by FPLC on a mono-S column to get pure Cro-protein. Finally the protein was dialysed with 50 mM Tris–HCl, 100 mM NaCl, and 5% glycerol buffer of pH 7.2 and confirmed by gel electrophoresis.

IAEDANS, containing a haloalkyl moiety along with a naphthalene ring, is a selective thiol-reactive fluorescent probe. During the reaction with the sulfhydryl group (S–H), the iodine group of IAEDANS is substituted and IAEDANS is converted into AEDANS. At near-neutral (physiological) pH proteins can be coupled with thiol groups selectively in the presence of amine groups. The site of reaction is at the introduced cysteine residues (Cys37) at the N-terminal half of the protein. Appropriate amounts of protein and IAEDANS were mixed in 50 mM Tris–HCl, 100 mM NaCl, and 5% glycerol buffer of pH 7.2 and left overnight in the dark and extensively dialysed with the same buffer before use.

DNA labeling with DAPI

The DAPI-operator DNA (O_R3/O_R2) solution was prepared by adding the requisite volume of probe solution (aqueous) to the corresponding DNA solution with continuous stirring for 4–5 hours in the dark.

Experimental details

All the experiments were performed at room temperature (~20 °C). All absorbance and fluorescence measurements were performed using a Shimadzu UV-2450 spectrophotometer and a Jobin Yvon Fluoromax-3 fluorimeter respectively. The excitation and emission band passes were 3 nm and 3 nm, respectively. The excitation wavelength was 350 nm and 375 nm for AEDANS and DAPI respectively.

Using the absorption technique and following the reported literature[13] we have calculated the labeling efficiency of the probe AEDANS towards the protein CroG37C. Using absorbance at 280 nm and 363 nm for protein and AEDANS, respectively, the labeling efficiency of AEDANS is found to be 86%, *i.e.* 0.86 mol AEDANS per mole of CroG37C monomer protein.

Picosecond-resolved fluorescence transients were measured by using a time correlated single photon counting system coupled with MCP-PMT from Life Spec-ps, Edinburgh Instruments, UK with a 70 ps instrument response function (IRF). It should be noted that we can resolve at least one quarter of the instrument response time

constants with our time resolved instrument after the de-convolution of the IRF. The excitation at 375 nm was obtained using a pulse laser diode from PicoQuant, Germany. The details of the time resolved fluorescence setup have been depicted in our previous reports.[26] The average lifetime (amplitude-weighted) of a multi-exponential decay is expressed as $\tau_{av} = \sum_{i=1}^{N} c_i\tau_i$. Time-resolved emission spectra (TRES) were used to determine time dependent fluorescence Stokes shifts following the methodologies reported earlier.[27] In brief, the normalized spectral shift correlation function or the solvent correlation function, $C(t)$, defined as, $C(t) = \frac{\nu(t) - \nu(\infty)}{\nu(0) - \nu(\infty)}$, where $\nu(0)$, $\nu(t)$, and $\nu(\infty)$ are the emission maxima (in cm^{-1}) at time 0, t, and ∞ respectively.[26] Time-resolved area normalised emission spectra (TRANES) were constructed following an earlier work.[28] For anisotropy measurements we collected the fluorescence transients keeping the emission polariser parallel and perpendicular to the excitation polariser and the anisotropy $r(t)$ of the different systems was calculated according to the equation $r(t) = \frac{I_{para} - G \times I_{perp}}{I_{para} + 2 \times G \times I_{perp}}$, where I_{para} and I_{perp} are the fluorescence emission intensities measured by keeping the polariser parallel and perpendicular to the excitation polariser respectively. G is the grating factor.[29]

Results and discussion

In order to investigate how the sequence-specific DNA binding modulates protein conformation and dynamics at or near the site of protein–DNA interaction in the N-terminal half of the Cro-protein, a cysteine was introduced through site-directed mutagenesis into the N-terminal half (G37C) of the protein which is in close proximity of the protein–DNA interface (Scheme 1). It has to be noted that the Glycine37 (G37) residue is not taking part in the Cro protein–operator DNA interaction.[30–32] The reaction of CroG37C with a sulfhydryl reactive fluorescent probe will label Cys37 exclusively due to the absence of cysteine residues in the wild-type Cro-protein. Labeling of the cysteine residue with IAEDANS (5-((((2-iodoacetyl)amino)ethyl)amino)naphthalene-1-sulfonic acid) to observe structural and dynamical properties of the protein surface is well documented in the contemporary literature.[13,33] The steady-state emission spectra of the AEDANS group in different systems are shown in Fig. 1a. A significant blue-shift in the emission spectrum (at 475 nm) of the probe in CroG37C with respect to that in an aqueous buffer solution (at 500 nm) indicates the shielded location of the probe in the CroG37C protein dimer (excitation at 350 nm). Further blue-shift in the emission spectra of AEDANS-CroG37C upon complexation with its two DNA binding sites, O_R3 and O_R2 (450 nm), compared to that of the probe in the free CroG37C confirms further shifting of the probe towards a less polar environment of the dimer protein molecule. The observation of no significant difference between the emission spectra of the probe in the O_R3–CroG37C and O_R2–CroG37C complexes is consistent with the fact that the immediate environment of the AEDANS remains similar in both the complexes.

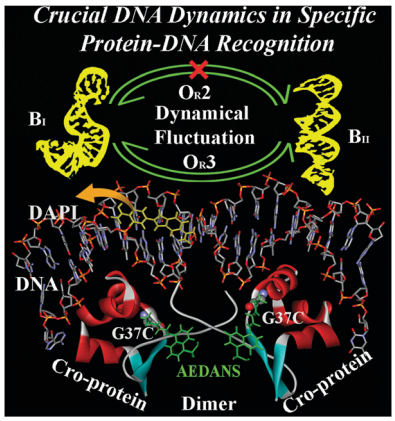

Scheme 1 Schematic representation of the Cro-protein dimer with two operator DNAs, O_R3 and O_R2. The domain fluctuation (interconversion of B_I to B_{II} and *vice versa*) of O_R3 upon complexation with the dimer is also highlighted (see text).

In order to obtain a molecular picture of rotational flexibility of the free and operator-bound protein, we have investigated the polarization gated fluorescence anisotropy of AEDANS in CroG37C in the absence and presence of O_R3 and O_R2 operator DNA as shown in Fig. 1b and c. Numerical fitting of fluorescence anisotropy of CroG37C protein with a multi-exponential decay function reveals time constants of 160 ps (95%) and 7 ns (5%). The estimated rotational time constant(s) for the tumbling motion of Cro-protein is estimated to be 7 ns using the Stokes–Einstein–Debye (SED) equation.[12,34] During the fitting we have fixed the longer time constant to be 7 ns. The different time constants indicate the different motions (local/global) of AEDANS attached to the Cys37 residue at the N-terminal half of the CroG37C protein. Upon complexation with O_R3 operator DNA the time constants become 500 ps (96%) and 7 ns (4%) as shown in Table 1. However, in the case of O_R2 complexation the time components are 390 ps (96%) and 7 ns (4%). This observation clearly indicates that the mobility of the AEDANS (bound to the cysteine residue) in the N-terminal half of CroG37C protein upon complexation with operator DNAs becomes restricted, may be due to the shifting of the probe into a more hydrophobic pocket of the protein, consistent with the observed anisotropy in the steady-state (data not shown). However, the flexibility of the AEDANS probe in the O_R2 operator DNA complex is comparatively higher than that in the O_R3 operator DNA complex. This may indicate substantial conformational differences between the two complexes. Overall, the results of the anisotropy decay experiments indicate that the residual motion at the N-terminal half of CroG37C in the complex is DNA sequence-specific.

For further investigation of the dynamics at the protein binding domain of the DNAs, we have labeled both the operator DNAs (O_R3 and O_R2) with DAPI (4′,6-diamidino-2-phenylindole), a well known minor groove binder.[25,35,36] Fig. 2a and b describe the emission spectra of DAPI bound to operator DNA in the presence and absence of wild-type Cro-protein (WT), along with the emission spectra of DAPI in an aqueous buffer solution.

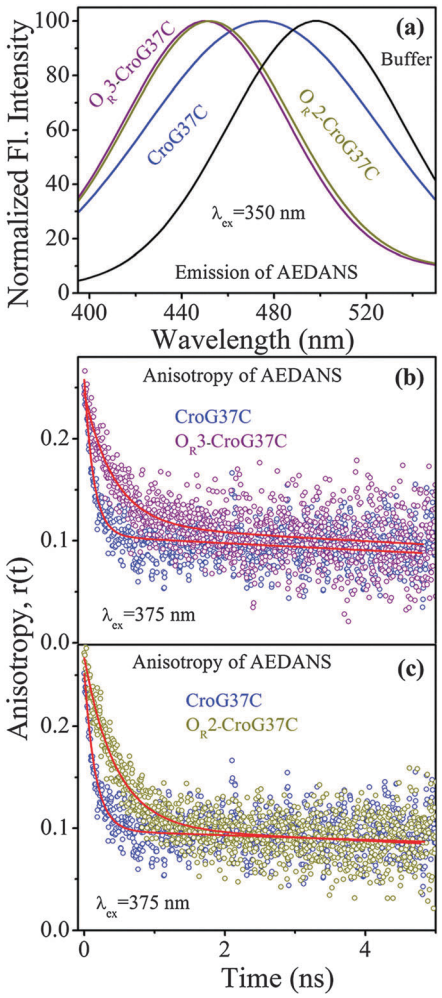

Fig. 1 (a) Steady-state emission spectra of fluorescent probe AEDANS in CroG37C, O_R3–CroG37C, O_R2–CroG37C, and buffer (excitation at 350 nm). Picosecond resolved fluorescence anisotropy decays of AEDANS in CroG37C, O_R3–CroG37C (b) and O_R2–CroG37C (c) are shown (excitation at 375 nm).

Table 1 Rotational time scales of AEDANS attached to the Cys37 residue in different systems

System	τ_1 (%) ns	τ_2 (%) ns
CroG37C	0.16 ± 0.03 (95%)	7.0 (5%)
O_R3–CroG37C	0.50 ± 0.04 (96%)	7.0 (4%)
O_R2–CroG37C	0.39 ± 0.02 (96%)	7.0 (4%)

In the presence of O_R3 (Fig. 2a) and O_R2 DNA (Fig. 2b), the emission maximum of DAPI (465 nm in buffer) is significantly blue shifted (O_R3 operator DNA: 448 nm, O_R2 operator DNA: 447 nm). In the presence of Cro-protein, the emission spectrum is further blue shifted in the case of the O_R3–Cro complex (442 nm), whereas it remains almost unaltered for the O_R2–Cro complex (445 nm). While the steady state anisotropy of DAPI bound to O_R3 remains almost constant, in the case of the O_R3–Cro complex the anisotropy decreases with the increase in detection wavelength as shown in Fig. 2c. The observation can be rationalized in the following two ways. Firstly, the probe DAPI could remain in two different environments namely DNA and bulk solution, revealing less anisotropy in the red edge of the emission spectrum. Another reason could be from a single emissive species of DAPI in DNA with different degrees of solvation[37] which could come from the dynamical flexibility of the probe containing the region of the DNA upon complexation of the Cro-protein. We have ruled out the former possibility by time-resolved area normalized emission spectroscopy (TRANES) as evident in the following section. However, in the case of the O_R2 operator DNA complex, the steady-state anisotropy of DAPI remains constant upon binding with Cro (Fig. 2d).

To investigate the conformational and structural change within the operator DNA itself in detail that occurs upon interaction with Cro-protein, time-resolved anisotropy studies of the probe DAPI were performed. Bi-exponential fitting of fluorescence anisotropy of DAPI in O_R3 operator DNA yielded time components of 80 ps (13%) and 5.83 ns (87%). Upon complexation of the DNA with Cro-protein, the faster time components became 40 ps (35%), as evident from Fig. 3a. However, in the case of O_R2 operator DNA the time constants were calculated to be 70 ps (15%) and 5.12 ns (85%) and they became 60 ps (24%) and 4.62 ns (76%) upon conjugation with Cro-protein (Fig. 3b) as shown in Table 2. To validate our results we have also fitted the parallel and perpendicular fluorescence decays individually by Spencer and Weber equations and obtained similar rotational time scales for the corresponding systems[38] consistent with those revealed from the fluorescence anisotropy decays. The observed rotational time constants of the anisotropy decay of the both operator DNAs are consistent with our earlier studies.[25] Our results indicate that the flexibility of the probe in the minor groove of the O_R3 operator DNA in the O_R3–Cro complex is higher compared to that of the O_R2–Cro complex, consistent with the steady-state anisotropy study. The decrease in the rotational time scales of the probe in the protein–operator DNA complex compared to that in the corresponding operator DNA clearly reflects higher dynamical flexibility of the operator DNA upon complexation with the repressor protein leading to the exposure of the probe DAPI to the aqueous environment.[39] In fact a significant bending of the protein binding region of O_R3 compared to O_R2 with the Cro-protein has been observed previously.[31,39,40] The increased flexibility of the binding region, where the probe DAPI is supposed to reside (middle portion of the operator DNA), in terms of mixture of B_I and B_{II} forms of the DNA has also been evidenced in the O_R3 operator.[23]

After obtaining the rotation time scales of DAPI, attached to the operator DNAs and the corresponding repressor complex, we have investigated the dynamical timescales of the Cro-protein binding domain of operator DNAs at the protein–DNA interface. Picosecond-resolved fluorescence transients of DAPI bound to operator DNAs in the absence and presence of Cro-protein have been measured at a number of wavelengths across the emission spectrum of DAPI in the complex. Fig. 4a and b show the decay transient of DAPI doped O_R3 operator DNA in the absence and presence of Cro-protein at two characteristic wavelengths (extreme blue and red end of the fluorescence spectrum), respectively.

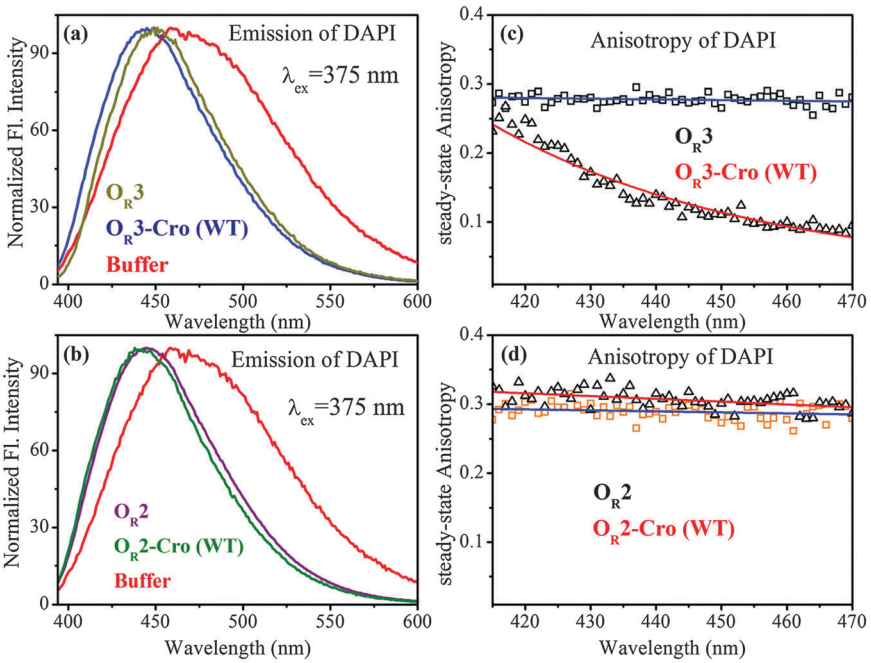

Fig. 2 Steady-state emission spectra of fluorescent probe DAPI in O_R3 and O_R3–Cro (wild type) (a) and O_R2 and O_R2–Cro (wild type) (b) are shown. Steady-state anisotropies of the probe DAPI in the corresponding systems are shown in (c) and (d) (excitation at 375 nm). The solid lines in (c) and (d) are guide to eyes.

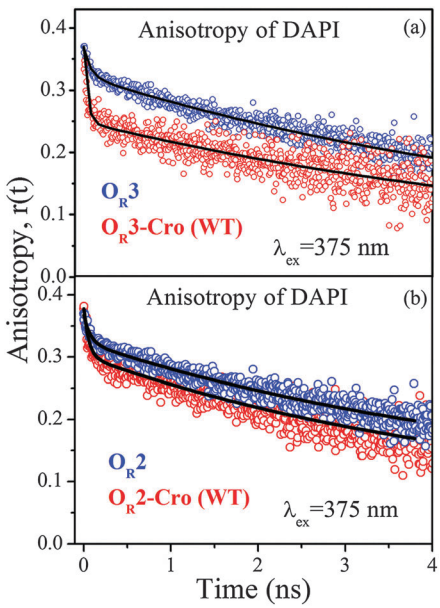

Fig. 3 Picosecond resolved fluorescence anisotropy decays of DAPI in O_R3 and O_R3–Cro (wild type) (a) and O_R2 and O_R2–Cro (wild type) (b) are shown.

Table 2 Rotational time scales of DAPI attached to O_R3/O_R2 operator DNA in different systems

System	τ_1 (%) ns	τ_2 (%) ns
O_R3	0.08 ± 0.01 (13%)	5.83 ± 0.2 (87%)
O_R3–Cro (WT)	0.04 ± 0.01 (35%)	6.19 ± 0.3 (65%)
O_R2	0.07 ± 0.02 (15%)	5.12 ± 0.1 (85%)
O_R2–Cro (WT)	0.06 ± 0.02 (24%)	4.62 ± 0.2 (63%)

An ultrafast decay component in the blue end is eventually converted into a rise component of a similar time constant in the red end for both the cases. The nature of the wavelength-dependent transients across the emission spectrum of the probe DAPI in the DNA and protein–DNA complex signifies solvation stabilization of the probe in the DNA environments.[26,41] Fig. 4c and d show the constructed time-resolved emission spectra (TRES) of DAPI with a spectral shift of 693 and 546 cm^{-1} for O_R3 operator DNA in the absence and presence of Cro-protein, respectively, in a 10 ns time window, which indicates that DAPI is stabilized due to solvation by its immediate environment in the excited state. Fig. 5a and b displays the transients of DAPI bound to O_R2 operator DNA in the absence and presence of Cro-protein respectively. The corresponding TRES are plotted in Fig. 5c and d with a spectral shift of 708 and 722 cm^{-1} in the 10 ns window for O_R2 operator DNA and the O_R2 operator DNA complex, respectively.

The solvation correlation function [$C(t)$] for both the DNA and its protein–DNA complex is plotted up to 10 ns as shown in Fig. 6a and b, revealing temporal excited-state energy relaxation of the fluorophore in the DNA environments. Two-component exponential decay fitting of $C(t)$ for O_R3 operator DNA yields time components of 0.18 (71%) and 2.0 ns (29%) and for the O_R3–Cro complex the time constants obtained are 30 ps (82%) and 1.55 ns (18%). However, in the case of O_R2 operator DNA and the O_R3–Cro complex the fitting reveals almost a similar kind of decay with time constants of 220 ps (66%) and 1.43 ns (34%), consistent with earlier reported results.[25] It has to be noted that due to limited time resolution, we are missing the

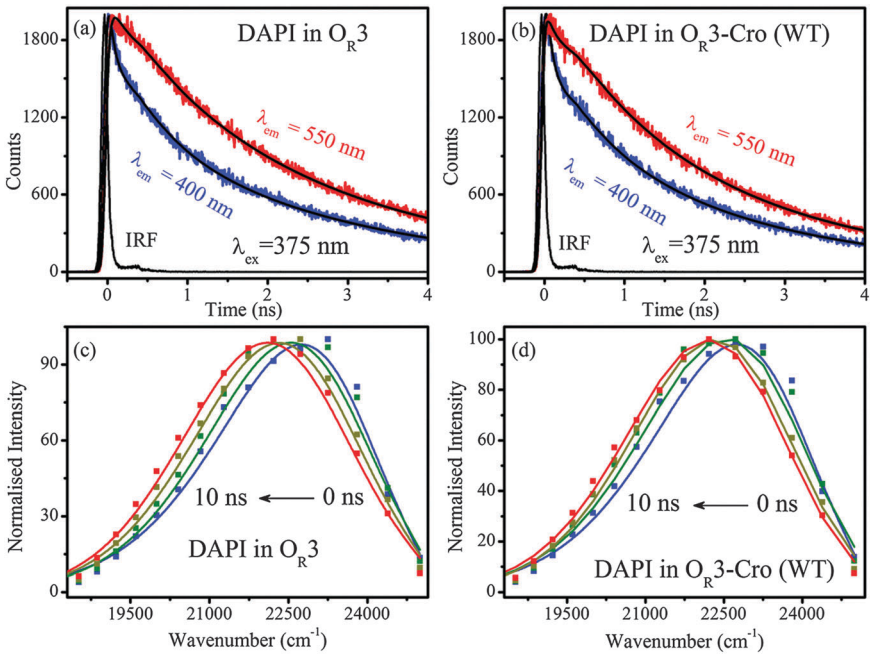

Fig. 4 Picosecond-resolved transient of DAPI at the blue and red end of the emission spectrum in (a) O_R3 and (b) O_R3–Cro (wild type) complex. Time-resolved emission spectra (TRES) of the corresponding systems are shown in (c) and (d).

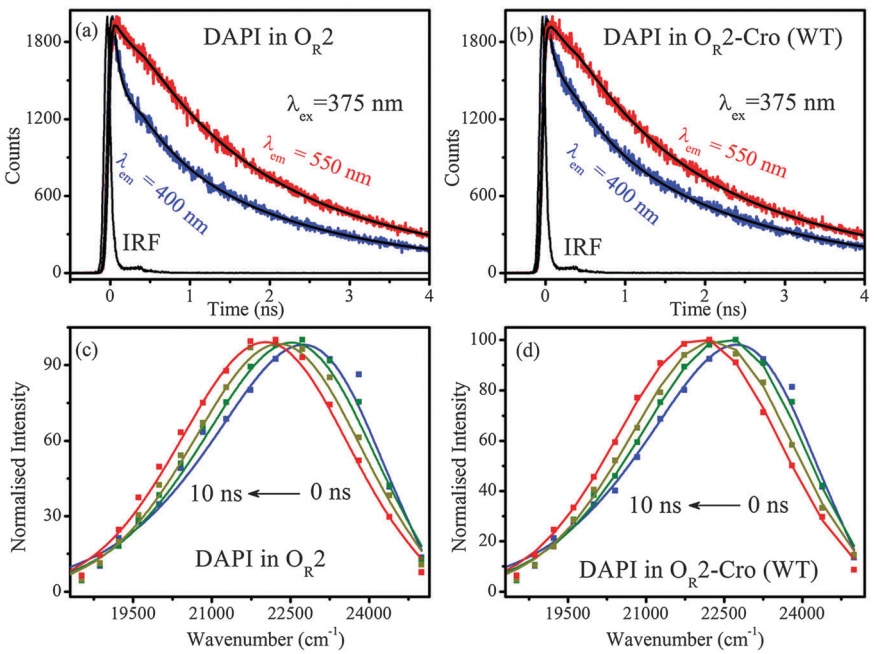

Fig. 5 Picosecond-resolved transient of DAPI at the blue and red end of the emission spectrum in (a) O_R2 and (b) O_R2–Cro (wild type) complex. Time-resolved emission spectra (TRES) of the corresponding systems are shown in (c) and (d).

~1 ps component of DNA minor groove water dynamics,[42,43] which is exclusively from bulk-type water in close proximity of the DNA surface. However, the observed sub-hundred to few hundred ps timescales are responsible for bound type water dynamics, associated with the DNA minor groove structure.[44] The longer nanosecond component is responsible for the relaxation of DNA structural fluctuation.[44] The observation suggests minimal perturbation in the minor groove of O_R2 operator DNA upon complexation with Cro-protein. However, in the case of O_R3 a significant faster component arises upon interaction with Cro-protein. The observation indicates that strong binding with Cro-protein allows the DNA to be more flexible compared to that with the O_R2, consistent with earlier studies.[20,30]

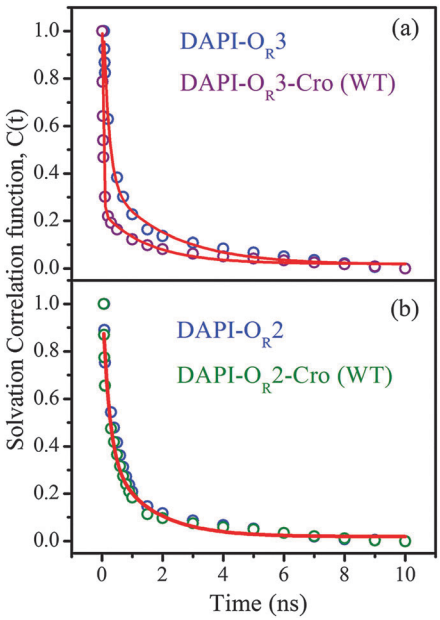

Fig. 6 Solvation correlation decay profiles of DAPI in O_R3 and O_R3–Cro (wild type) (a) and O_R2 and O_R2–Cro (wild type) (b) are shown.

It has to be noted that the faster component of both time resolved anisotropy and solvation of the probe DAPI in O_R3 upon complexation with Cro-protein could be rationalized in terms of DAPI population in DNA and bulk water contributing heterogeneous time scales. In order to rule out the possibility we have performed TRANES analysis of the TRESs of the DAPI in the operator DNAs before and after complexation with the Cro-protein. As reported earlier TRANES analysis which offers an iso-emissive point in the area normalized TRES could be an excellent tool to conclude the presence of two emissive species in the excited state of a molecule.[28,45] Careful analysis of the TRANES of the probe DAPI in the operator DNAs before and after the complexation with the Cro-protein does not show any iso-emissive point ruling out the possibility of two emitting species in the case of DAPI in O_R3 with the Cro-protein. Thus the faster time scales in the physical motion (anisotropy) and environmental dynamics (solvation) of the probe DAPI clearly reveal enhanced dynamical flexibility of the protein binding region of the operator DNA O_R3 compared to that of the operator O_R2. The overall picture that comes from our present experimental studies is shown in Scheme 1.

Conclusion

Till date, what determines the affinities of DNA-binding proteins for their target sequences is only understood in a broad sense. The least understood aspect is the entropic contributions which may fine-tune the affinity for different target sites. The entropic contributions may be in the form of conformational entropy of bound protein or DNA, the entropy of solvent molecules associated with proteins and DNA or the entropy of ion-release associated with the DNA or the protein. Even small changes in any of these components may alter the binding affinities enough to alter biological outcomes. Thus, it is important to understand the motional characteristics of proteins, DNAs and their respective hydration layers in different protein–DNA complexes. Cro-protein binds to O_R3 with approximately 3 kcal mole^{-1} more binding energy than that of the O_R2.[46] Cro-protein association with O_R3 is entropy driven, suggesting a significant role of the entropic component. Significant reduction of DNA relaxation time upon Cro binding to O_R3, as reported here, suggests an increase in DNA-domain entropy upon complex formation. Interestingly, such a reduction is not apparent in the case of O_R2, indicating that there may be a differential entropic stabilization of the O_R3 complex with respect to the O_R2 complex. At least a part of the differential affinity between O_R3 and O_R2 may be accounted for by such DNA-domain dynamics.

In brief, we suggest that recognition of different DNA sequences by a transcription factor not only involves different interaction patterns of protein atoms with that of the DNA atoms, but the motional freedom of the macromolecules also undergoes significant changes. We propose that a full understanding of protein–DNA recognition must involve elucidation of the entropic character of the participating macromolecules and protein binding domains of the operator DNAs.

Acknowledgements

SC and BG thank the CSIR, India, for the research fellowships. SR acknowledges J. C. Bose Fellowship from DST (India). We thank DST (India) for financial grant (SB/S1/PC-011/2013) and DAE (India) for support (2013/37P/73/BRNS).

References

1 S. A. Teichmann and M. M. Babu, *Nat. Genet.*, 2004, **36**, 492–496.
2 D. S. Johnson, A. Mortazavi, R. M. Myers and B. Wold, *Science*, 2007, **316**, 1497–1502.
3 A. Manglik and B. Kobilka, *Curr. Opin. Cell Biol.*, 2014, **27**, 136–143.
4 M. Shiina, K. Hamada, T. Inoue-Bungo, M. Shimamura, A. Uchiyama, S. Baba, K. Sato, M. Yamamoto and K. Ogata, *J. Mol. Biol.*, 2015, **427**, 1655–1669.
5 J. A. Lefstin and K. R. Yamamoto, *Nature*, 1998, **392**, 885–888.
6 H. N. Motlagh, J. O. Wrabl, J. Li and V. J. Hilser, *Nature*, 2014, **508**, 331–339.
7 R. Nussinov, C.-J. Tsai and J. Liu, *J. Am. Chem. Soc.*, 2014, **136**, 17692–17701.
8 N. Popovych, S. Sun, R. H. Ebright and C. G. Kalodimos, *Nat. Struct. Mol. Biol.*, 2006, **13**, 831–838.
9 J. Monod, J. Wyman and J.-P. Changeux, *J. Mol. Biol.*, 1965, **12**, 88–118.
10 S.-R. Tzeng and C. G. Kalodimos, *Nature*, 2009, **462**, 368–372.
11 S. Batabyal, S. Choudhury, D. Sao, T. Mondol and S. Kumar Pal, *Biomol. Concepts*, 2014, **5**, 21–43.

12 T. Mondol, S. Batabyal, A. Mazumder, S. Roy and S. K. Pal, *FEBS Lett.*, 2012, **586**, 258–262.
13 S. Choudhury, G. Naiya, P. Singh, P. Lemmens, S. Roy and S. K. Pal, *ChemBioChem*, 2016, **17**, 605–613.
14 T. Mondol, S. Batabyal and S. K. Pal, *J. Bimol. Struct. Dyn.*, 2012, **30**, 362–370.
15 S. Batabyal, T. Mondol, S. Choudhury, A. Mazumder and S. K. Pal, *Biochimie*, 2013, **95**, 2168–2176.
16 Y. Levy and J. N. Onuchic, *Annu. Rev. Biophys. Biomol. Struct.*, 2006, **35**, 389–415.
17 D. U. Ferreiro, I. E. Sánchez and G. de Prat Gay, *Proc. Natl. Acad. Sci. U. S. A.*, 2008, **105**, 10797–10802.
18 Y. Yang, Y. Qin, Q. Ding, M. Bakhtina, L. Wang, M.-D. Tsai and D. Zhong, *Biochemistry*, 2014, **53**, 5405–5413.
19 S. Choudhury, S. Batabyal, P. K. Mondal, P. Singh, P. Lemmens and S. K. Pal, *Chem. – Eur. J.*, 2015, **21**, 16172–16177.
20 Y. L. Lyubchenko, L. S. Shlyakhtenko, E. Appella and R. E. Harrington, *Biochemistry*, 1993, **32**, 4121–4127.
21 C. Karslake, M. V. Botuyan and D. G. Gorenstein, *Biochemistry*, 1992, **31**, 1849–1858.
22 M. Trieb, C. Rauch, B. Wellenzohn, F. Wibowo, T. Loerting and K. R. Liedl, *J. Phys. Chem. B*, 2004, **108**, 2470–2476.
23 J. D. Baleja and B. D. Sykes, *Biochem. Cell Biol.*, 1994, **72**, 95–108.
24 P. J. Darling, J. M. Holt and G. K. Ackers, *Biochemistry*, 2000, **39**, 11500–11507.
25 D. Banerjee and S. K. Pal, *J. Phys. Chem. B*, 2008, **112**, 1016–1021.
26 S. Choudhury, S. Batabyal, T. Mondol, D. Sao, P. Lemmens and S. K. Pal, *Chem. – Asian J.*, 2014, **9**, 1395–1402.
27 M. L. Horng, J. A. Gardecki, A. Papazyan and M. Maroncelli, *J. Phys. Chem.*, 1995, **99**, 17311–17337.
28 A. Koti, M. Krishna and N. Periasamy, *J. Phys. Chem. A*, 2001, **105**, 1767–1771.
29 P. Singh, S. Choudhury, G. K. Chandra, P. Lemmens and S. K. Pal, *J. Photochem. Photobiol., B*, 2016, **157**, 105–112.
30 R. G. Brennan, S. L. Roderick, Y. Takeda and B. W. Matthews, *Proc. Natl. Acad. Sci. U. S. A.*, 1990, **87**, 8165–8169.
31 W. Anderson, D. Ohlendorf, Y. Takeda and B. Matthews, *Nature*, 1981, **290**, 754–758.
32 Y. Takeda, A. Sarai and V. M. Rivera, *Proc. Natl. Acad. Sci. U. S. A.*, 1989, **86**, 439–443.
33 J. Fang, A. Mehlich, N. Koga, J. Huang, R. Koga, X. Gao, C. Hu, C. Jin, M. Rief and J. Kast, *Nat. Commun.*, 2013, **4**, 2974–2983.
34 T. Köddermann, R. Ludwig and D. Paschek, *ChemPhysChem*, 2008, **9**, 1851–1858.
35 J. Riedl, R. Pohl, N. P. Ernsting, P. Orság, M. Fojta and M. Hocek, *Chem. Sci.*, 2012, **3**, 2797–2806.
36 J. Kapuscinski, *Biotech. Histochem.*, 2009, **70**, 220–233.
37 A. Chattopadhyay, A. Arora and D. A. Kelkar, *Eur. Biophys. J.*, 2005, **35**, 62–71.
38 D. O'Connor, *Time-correlated single photon counting*, Academic Press, 2012.
39 D. A. Erie, G. Yang, H. C. Schultz and C. Bustamante, *Science*, 1994, **266**, 1562–1566.
40 C. Torigoe, S.-i. Kidokoro, M. Takimoto, Y. Kyogoku and A. Wada, *J. Mol. Biol.*, 1991, **219**, 733–746.
41 S. Choudhury, P. K. Mondal, V. K. Sharma, S. Mitra, V. G. Sakai, R. Mukhopadhyay and S. K. Pal, *J. Phys. Chem. B*, 2015, **119**, 10849–10857.
42 S. K. Pal, L. Zhao and A. H. Zewail, *Proc. Natl. Acad. Sci. U. S. A.*, 2003, **100**, 8113–8118.
43 S. K. Pal, L. Zhao, T. Xia and A. H. Zewail, *Proc. Natl. Acad. Sci. U. S. A.*, 2003, **100**, 13746–13751.
44 E. B. Brauns, M. L. Madaras, R. S. Coleman, C. J. Murphy and M. A. Berg, *J. Am. Chem. Soc.*, 1999, **121**, 11644–11649.
45 S. Rakshit, R. Saha, P. K. Verma and S. K. Pal, *Photochem. Photobiol.*, 2012, **88**, 851–859.
46 P. J. Darling, J. M. Holt and G. K. Ackers, *J. Mol. Biol.*, 2000, **302**, 625–638.

